

UM-TH-95-11
SPhT Saclay T95/049
hep-ph/9505378
September 11, 2018

Exclusive Semi-Leptonic Decays of b-Baryons into Protons

Will Loinaz¹

*Randall Laboratory of Physics,
University of Michigan, Ann Arbor, MI 48109-1120, USA*

R. Akhoury²

*CEA Service de Physique Theorique, CE-Saclay
F-91191 Gif-sur-Yvette, CEDEX, France*

Abstract

We present a QCD-based calculation of the exclusive semileptonic decay $\Lambda_b \rightarrow p l \bar{\nu}_l$. Using the ideas of Heavy Quark Effective Theory, we discuss the factorization of the amplitude. Further, resummed Sudakov effects are put in to ensure a consistent perturbative expansion.

¹E-mail: loinaz@walden.physics.lsa.umich.edu

²On sabbatical leave from the University of Michigan, Ann Arbor

The study of b-hadron decays has been the subject of considerable interest in recent years, as a source of information about CKM matrix elements, [1] as a laboratory for the application of QCD [2, 3, 4, 6] and the development of theoretical tools such as Heavy Quark Effective Theory (HQET)[5]. In particular, heavy-to-light decays are interesting because they give information on V_{ub} , but they are especially difficult to calculate because of the essential presence of strong interactions in the hadronic bound state. Recently, however, in [4] a method has been formulated for analyzing the exclusive decay $B^0 \rightarrow \pi l^+ \nu_l$ in the region of large hadronic recoil and in the limit of a very heavy b-quark. The approach combines HQET, perturbative factorization theorems for exclusive processes [8], and exponentiation of Sudakov double-logarithms [7]. In this paper we extend this technology to study the exclusive decay $\Lambda_b \rightarrow p l \bar{\nu}_l$, also in the limit of large hadronic recoil and large b quark mass. In this limit, the method provides an asymptotic regime in which a systematic expansion exists with corrections $\mathcal{O}(\alpha_s(c\Lambda_{QCD}m_b))$, where c is a calculable constant. For some recent model-dependent calculations of Λ_b decays, see [9]. From the phenomenological side,to the extent that the very large m_b limit is realistic our calculation is motivated by the possibility that it could provide another method for extracting V_{ub} from data, complementary to the B-meson studies. In addition, comparison of experiment with the predictions of our calculation will afford added insight into the applicability of perturbative QCD (PQCD) in processes with momentum transfers in the few-GeV range. Further, the analysis of this paper is useful for contrasting the decays $\Lambda_b \rightarrow p l \bar{\nu}_l$ and $B^0 \rightarrow \pi l^+ \nu_l$, which may be helpful in elucidating the surprisingly large difference in the Λ_b and B^0 lifetimes recently seen in experimental data [10].

We stress that in this paper we are calculating the purely perturbative contribution to the above-mentioned exclusive decay. This would be the dominant one in the limit of a very heavy b-quark. However, for realistic values of m_b there are could be sizable nonperturbative contributions in the form of higher-twist effects . These will be discussed in a future work [15]. However, as we shall see below, numerical indications are that a modified perturbation expansion is self-consistent even for realistic values of m_b .

The physical picture of this decay is similar to that for the meson, described in [4]. Sitting inside the Λ_b , the b-quark decays into a W^- and a fast-moving, nearly on-shell u-quark. The u-quark propagates through the remaining hadronic medium, picking up a light ud pair over a distance y . Since we are considering an exclusive decay, no gluon radiation escapes. If y were large enough ($\mathcal{O}(\frac{1}{\Lambda_{QCD}})$) we would expect considerable gluon radiation. Thus, for exclusive processes we expect the outgoing u-quark to propagate only small distances ($<< \mathcal{O}(\frac{1}{\Lambda_{QCD}})$) before acquiring a ud pair to form the color singlet which will hadronize to form the proton. Then the hard gluons which kick these spectator quarks will typically be off-shell by $\mathcal{O}(\Lambda_{QCD}m_b)$, large enough that we might expect perturbative factorization theorems to apply.

We will state the arguments and results of our approach and sketch the calculations. The calculational details will be published elsewhere [15]. Our procedure is to judiciously combine elements of [4] and [11, 12]. We first identify the sources of long-distance behaviour which must be dealt with in order to successfully apply perturbation theory. Soft divergences will arise from interactions of soft gluons with the heavy quark, and soft and collinear divergences will arise from the interactions of virtual partons travelling in the direction of the outgoing proton. As in [4], we separate out the soft divergences due to the heavy quark

using an eikonal treatment of the b-gluon interactions. All the other divergences we regulate using the Sudakov resummation procedure developed in [13] and applied to exclusive decays in [11, 12]. Of course these do not include the collinear divergences that are collected into the universal proton wavefunction. This modification of the perturbative expression takes into account the transverse momenta of the partons inside the proton. The resummation of the most important contribution behaves like $\exp[-\text{const} \times \log Q(\log(\frac{\log Q}{\log b}))]$ in the leading logarithmic approximation where b is the conjugate Fourier transform variable to l_\perp . In the above Q is a typical momentum transfer which is of the order of m_b in our case. This Sudakov suppression selects the components of the proton wavefunction with small transverse separation, thereby ensuring that the exchanged hard gluon is always offshell and consequently perturbation theory for the hard scattering amplitude remains stable and reliable. Contributions from additional non-valence Fock states will be suppressed by $\mathcal{O}(\frac{\Lambda_{QCD}}{m_b})$ from standard parton model considerations for hard exclusive processes [8].

We conclude by calculating the form factor and differential decay rate, combining our form factor with model Λ_b and proton wavefunctions.

We now discuss the factorization of the hadronic form factor. The interaction Hamiltonian relevant to the decay $\Lambda_b \rightarrow p l \bar{\nu}_l$ is

$$H_{int} = \frac{G_F}{\sqrt{2}} V_{ub} (\bar{u} \gamma_\mu (1 - \gamma_5) b) (\bar{l} \gamma^\mu (1 - \gamma_5) \nu_l) \quad (1)$$

The amplitude is

$$\mathcal{M} = \frac{G_F}{\sqrt{2}} V_{ub} \underbrace{\langle P(p') | \bar{u} \gamma_\mu (1 - \gamma_5) b | \Lambda_b(p) \rangle}_{M_\mu} (\bar{l} \gamma^\mu (1 - \gamma_5) \nu_l) \quad (2)$$

We will be concerned with calculating the hadronic matrix element M_μ in the limit of $x \sim 1$, where x is defined by

$$x = \frac{2p \cdot p'}{m_b^2} \quad (3)$$

where p is the momentum of the Λ_b and p' is that of the outgoing proton, which we take to be in the (+) direction. In [4] it was shown that for $B^0 \rightarrow \pi l^+ \nu_l$ the hadronic matrix element could be sensibly written as a convolution of a hard-scattering amplitude with initial- and final- state valence hadronic wavefunctions. For the present case the analogous treatment is valid. As we discuss below, we can write (suppressing color and spinor indices):

$$M_\mu(p, p') = \int \frac{d^4 k_2}{(2\pi)^4} \frac{d^4 k_3}{(2\pi)^4} \mathcal{A}_\mu(p, p') \Psi_{\Lambda_b}(p, k_2, k_3) \quad (4)$$

where k_2 and k_3 are light quark initial momenta, Ψ_{Λ_b} is the Λ_b valence wavefunction, and \mathcal{A}_μ is itself a convolution of the hard-scattering amplitude, H_μ , and the proton valence wavefunction, $\bar{\Psi}_P$. Written explicitly,

$$M_\mu(p, p') = \int_0^1 [d\xi_i] \int [d^2 l_\perp] \int \frac{d^4 k_2}{(2\pi)^4} \frac{d^4 k_3}{(2\pi)^4} \bar{\Psi}_P(\xi_i, p', l_\perp) H_\mu(\xi_i, l_\perp, p', p, k_2, k_3) \Psi_{\Lambda_b}(p, k_2, k_3) \quad (5)$$

$$[d\xi_i] = \delta \left(1 - \sum_{i=1}^3 \xi_i \right) d\xi_1 d\xi_2 d\xi_3 \quad (6)$$

$$[d^2 l_{\perp}] = \delta^2 \left(\sum_{i=1}^3 l_{\perp i} \right) d^2 l_{\perp 1} d^2 l_{\perp 2} d^2 l_{\perp 3} \quad (7)$$

where the ξ_i are the longitudinal momentum fractions of the proton's valence quarks and $l_{\perp i}$ are the corresponding perp components.

We now briefly outline the steps leading to eqn.[4]. As usual in the treatment of exclusive processes, to yield a hard-scattering amplitude computable in PQCD the infrared divergences must be factored from the hard-scattering amplitude into the wavefunctions. The factorization procedure is a straightforward extension of the corresponding analysis in [4]. We review the salient points of the factorization of soft divergences here. The remaining collinear divergences will be controlled by the resummation procedure discussed later.

Step 1 Decoupling assumption: integrate out the heavy b-quark loop effects, allowing the matrix element to be written as

$$M_{\mu} = \langle P(p') | J_{\mu}(0) | \Lambda_b \rangle_{\mathcal{L}_{QCD}} = \langle P(p') | T(J_{\mu}(0) V(A^0)) | \Lambda_b \rangle_{\mathcal{L}(q)} \quad (8)$$

Here V represents a single b-quark line connected to the weak vertex. V is composed of a sequence of b-gluon vertices and b-propagators and as such contains the full effect of the terms of the Lagrangian $\mathcal{L}_0(b) - ig\bar{b}\gamma \cdot Ab$, up to loop corrections. It is V which now contains the soft divergences. Note that the matrix element is now calculated using the light-quark Lagrangian density $\mathcal{L}(q)$ only.

Step 2 Go to the Λ_b rest-frame and introduce the eikonal phase.

$$U(A^0) = \mathcal{P}exp[-ig \int_{-\infty}^0 n \cdot A(\lambda n_{\mu}) d\lambda] \quad (9)$$

n is a unit vector in the direction of the heavy-quark velocity (here $n_{\mu} = \delta_{0\mu}$). This contains precisely the soft divergences of $V(A^0)$ that we wish to remove. The associated Feynman rule is shown explicitly in [4].

Step 3 Define a subtracted b-quark line, $V^{fin} = VU^{-1}$, from which the soft divergences have been removed. To lowest order this is the difference between the full b-quark propagator and the eikonal propagator.

Step 4 Express the hadronic matrix element in terms of this subtracted propagator, inserting a UU^{-1} and a sum over a complete set of states to obtain:

$$M_{\mu} = \sum_{n=3}^{\infty} \langle P(p') | T(J_{\mu}(0) V^{fin}(A^0) \otimes_n U(A^0)) | \Lambda_b \rangle_{\mathcal{L}(q)} \quad (10)$$

Here the $\sum_{n=3}^{\infty} \dots \otimes_n \dots$ denotes a summation over intermediate states with $n-1$ light partons, integration over their momenta, and summation over other relevant indices.

Step 5 Neglect the higher Fock states. What remains after a reorganization of the perturbative sum is:

$$M_\mu = \int \frac{d^4 k_2}{(2\pi)^4} \frac{d^4 k_3}{(2\pi)^4} \sum_{n=3}^{\infty} [\langle P(p') | T(J_\mu(0) V^{fin}(A^0)) | bud \rangle \langle bud | U(A^0) | \Lambda_b \rangle]_{\mathcal{L}(q)} \quad (11)$$

where we identify the second factor in the integrand as the Λ_b wavefunction and the first factor as \mathcal{A}_μ from eqn (3). The passage to eqn (4) is justified if the process the proton emerges from a short-distance region and the procedure is by now fairly standard (see [12]).

We next discuss the implementation of the Sudakov suppression a la' Li and Sterman. For this purpose, following [11, 12] we work in an axial gauge. The first step is to transform eqn (4) into 'b' space, which is Fourier-conjugate to l_\perp :

$$M_\mu(p, p') = \int_0^1 [d\xi_i] \int [d^2 b] \int \frac{d^4 k_2}{(2\pi)^4} \frac{d^4 k_3}{(2\pi)^4} \mathcal{P}_p(\xi_i, p', b_i, \mu) H_\mu(\xi_i, p', p, k_2, k_3, b_i, \mu) \Psi_{\Lambda_b}(p, k_2, k_3) \quad (12)$$

where

$$[d^2 b] = \frac{d^2 b_2}{(2\pi)^2} \frac{d^2 b_3}{(2\pi)^2} \quad (13)$$

μ is the factorization scale, and $\mathcal{P}_p(\xi_i, p', b_i, \mu)$ are the transformed proton wavefunctions. The \mathcal{P} s include all the large logarithmic and double logarithmic radiative corrections at large b . These have been resummed and exponentiated [13] and result in a suppression of the distribution amplitude at large b . Explicitly, we write

$$\mathcal{P}_p(\xi_i, p', b_i, \mu) = \exp \left[- \sum_{l=1}^3 \left(s(\xi_l, \tilde{b}_l, m_b) + \int_{\frac{1}{\tilde{b}_l}}^\mu \frac{d\bar{\mu}}{\bar{\mu}} \gamma_q(g^2(\bar{\mu})) \right) \right] \bar{\Psi}_P(\xi_i, p', w) + \mathcal{O}(\alpha_s^2(w)) \quad (14)$$

where $w = \min_i(\frac{1}{\tilde{b}_i})$. The $s(\xi_l, \tilde{b}_l, m_b)$ are defined in [13, 12] and $\gamma_q = -\frac{\alpha_s}{\pi}$ is the axial gauge quark anomalous dimension. The \tilde{b}_l are the infrared cutoff parameters and we follow the "MAX" prescription of [14], i.e.

$$\tilde{b}_l = \max[b_1, b_2, b_3] \quad (15)$$

where $b_1 = |b_2 - b_3|$. Including the μ dependence of the hard- scattering amplitude we can write our final result in the form

$$\begin{aligned} M_\mu(p, p') = & \frac{1}{(2\pi)^3} \int_0^1 [d\xi_i] \int_0^\infty b_2 db_2 \int_0^\infty b_3 db_3 \int_0^{2\pi} d\theta \int \frac{d^4 k_2}{(2\pi)^4} \frac{d^4 k_3}{(2\pi)^4} \\ & \bar{\Psi}_P(\xi_i, p', w) H_\mu(\xi_i, b_i, \theta, p', p, k_2, k_3, t_{\alpha_1}, t_{\alpha_2}) \Psi_{\Lambda_b}(p, k_2, k_3) \\ & \times \exp \left[-S(\xi_i, \tilde{b}_i, m_b, \tilde{t}_{\alpha_1}, \tilde{t}_{\alpha_2}) \right] \end{aligned} \quad (16)$$

where θ is the angle between b_2 and b_3 . In the above, $t_{\alpha_1}, t_{\alpha_2}$ are the appropriate scales at which the running couplings in the hard scattering amplitude are evaluated and are related

to the largest mass scales appearing in H_μ . The detailed forms are given below. The S are generically of the form

$$S = \sum_{l=1}^3 \left[s(\xi_l, \tilde{b}_l, m_b) - \int_{\frac{1}{\tilde{b}_l}}^{\tilde{t}_l} \frac{d\bar{\mu}}{\bar{\mu}} \gamma_q(g^2(\bar{\mu})) \right] \quad (17)$$

where the \tilde{t}_l depend on the hard scattering diagram (see below).

We now express the wavefunctions in explicit forms more useful for calculations. In the above we have neglected any intrinsic l_\perp dependence in the wavefunctions. A more complete treatment taking this into account will be given elsewhere [15]. We work in the rest frame of the Λ_b with the proton moving off in the (+) direction. Following the notation of other authors [16, 17] we write the final-state proton wavefunction:

$$\begin{aligned} \bar{\Psi}_P(\xi_i)_{\alpha\beta\gamma,lmn} &= \frac{1}{6} \epsilon_{lmn} \frac{1}{4} f_P [(C\gamma \cdot p')_{\alpha\beta} (\bar{u}_P(p')\gamma_5)_\gamma V(\xi_1, \xi_2, \xi_3) \\ &\quad + (C\gamma \cdot p' \gamma_5)_{\alpha\beta} \bar{u}_P(p')_\gamma A(\xi_1, \xi_2, \xi_3) \\ &\quad + (iC\sigma_{\delta\omega} p'_\omega) (\bar{u}_P(p')\gamma_\delta \gamma_5)_\gamma T(\xi_1, \xi_2, \xi_3)] \end{aligned} \quad (18)$$

$$= \int \prod_{i=1}^3 \left(\frac{d(z_i \cdot p')}{(2\pi)} e^{ik_i \cdot z_i} \right) \langle P(p') | \bar{u}_\alpha^l(z_1) \bar{u}_\beta^m(z_2) \bar{d}_\gamma^n(z_3) | 0 \rangle \quad (19)$$

where

$$2T(\xi_1, \xi_2, \xi_3) = \phi_P(\xi_1, \xi_3, \xi_2) + \phi_P(\xi_2, \xi_3, \xi_1) \quad (20)$$

$$2V(\xi_1, \xi_2, \xi_3) = \phi_P(\xi_1, \xi_2, \xi_3) + \phi_P(\xi_2, \xi_1, \xi_3) \quad (21)$$

$$2A(\xi_1, \xi_2, \xi_3) = \phi_P(\xi_2, \xi_1, \xi_3) - \phi_P(\xi_1, \xi_2, \xi_3) \quad (22)$$

and $\xi_1 + \xi_2 + \xi_3 = 1$. C is the charge conjugation operator and $\sigma_{\mu\nu} = \frac{i}{2}[\gamma_\mu, \gamma_\nu]$. f_P is related to the wavefunction at the origin. It is chosen such that the distribution amplitude has normalization $\int_0^1 [d\xi_i] \phi_P(\xi_i, \mu^2) = 1$.

We may define the Λ_b wavefunction similarly:

$$\Psi_{\Lambda_b}(k_2, k_3)_{\alpha\beta\gamma,lmn} = \frac{1}{6} \epsilon_{lmn} \left[[(\gamma \cdot p + m_b) \gamma_5 C]_{\beta\gamma} u(p)_\alpha \psi(p, k_2, k_3) \right] \quad (23)$$

$$= \int d^4 z_2 e^{ik_2 \cdot z_2} \int d^4 z_3 e^{ik_3 \cdot z_3} \langle 0 | b_\alpha^l(0) U(A^0) u_\beta^m(z_2) d_\gamma^n(z_3) | \Lambda_b(p) \rangle \quad (24)$$

Note that our choice of a scalar momentum wavefunction $\psi(p, k_2, k_3)$ (rather than a more complicated tensor structure) corresponds to an assumption of decoupling of the spin and orbital degrees of freedom in the light-quark system, as discussed in [18].

With our choice of frame we find that to leading order in m_b the only nontrivial dependence of the hard-scattering amplitude on k_2 and k_3 is through their (−) components. Thus it is convenient to define a distribution amplitude $\tilde{\phi}(k_2^-, k_3^-)$ which replaces $\psi(p, k_2^-, k_3^-)$ and in which the (+) and (⊥) components have been integrated out:

$$\tilde{\phi}(k_2^-, k_3^-) = \int \frac{dk_2^+ d^2 k_{2\perp}}{(2\pi)^4 \sqrt{2}} \int \frac{dk_3^+ d^2 k_{3\perp}}{(2\pi)^4 \sqrt{2}} \psi(p, k_2, k_3) \quad (25)$$

where $k_i^\pm = k_i^0 \pm k_i^3$. It is convenient to change to the dimensionless variables ξ, η defined by $\xi = \frac{k_2^-}{k_2^- + k_3^-}$ and $\eta = \frac{k_2^- + k_3^-}{m_b}$. In terms of these variables we normalize the distribution amplitude $\phi(\xi, \eta)$ by

$$\int_0^1 d\xi \int_0^1 \eta d\eta \phi(\xi, \eta) = 1 \quad (26)$$

and define f_{Λ_b} analogous to f_p :

$$\Psi_{\Lambda_b}(\xi, \eta)_{\alpha\beta\gamma, lmn} = \frac{1}{6} \epsilon_{lmn} \left[\frac{1}{4} f_{\Lambda_b} [(\gamma \cdot p + m_b) \gamma_5 C]_{\beta\gamma} u(p)_\alpha \phi(\xi, \eta) \right] \quad (27)$$

Thus, f_{Λ_b} is related to the Λ_b wavefunction at the origin to leading order in $\alpha_s(m_b^2)$. The higher order effects can be discussed; see [19] for the meson case. Using the above definitions and evaluating the traces, the Dirac structure of the leading terms will be of form $[\bar{u}_P(p') \gamma_\mu (1 - \gamma_5) u_{\Lambda_b}(p)]$. The matrix element may then be written (with color indices and color wavefunctions suppressed):

$$\begin{aligned} M_\mu &= \frac{1}{2} \frac{1}{(2\pi)^3} \left(\frac{1}{4} \right)^2 f_{\Lambda_b} f_P [\bar{u}_P(p') \gamma_\mu (1 - \gamma_5) u_{\Lambda_b}(p)] \times \\ &\quad \int_0^1 [d\xi_i] \int_0^1 \eta d\eta \int_0^1 d\xi \int_0^\infty b_2 db_2 \int_0^\infty b_3 db_3 \int_0^{2\pi} d\theta \bar{H}(\xi_i, \eta, \xi, b_2, b_3, \theta, p', p, t_{\alpha_1}, t_{\alpha_2}) \times \\ &\quad e^{-S} \phi(\xi, \eta) \end{aligned} \quad (28)$$

$$= [\bar{u}_P(p') \gamma_\mu (1 - \gamma_5) u_{\Lambda_b}(p)] F(x). \quad (29)$$

Explicit expressions for $\bar{H} e^{-S}$ for the different diagrams are given below. Note that the proton wavefunctions are included in the definition of \bar{H} .

We now discuss the calculation of the hard-scattering amplitude, H_μ . Unlike the $B^0 \rightarrow \pi l^+ \nu_l$ case, for $\Lambda_b \rightarrow p l \bar{\nu}_l$ only a small subset of the full set of 16 tree-level diagrams contribute to leading order in m_b . In a spacelike axial gauge with the gauge-fixing vector having no perp component, the leading diagrams are those shown in figure [1]. After contracting all spinor indices with the wavefunction spin-projection operators and all color indices to give initial- and final- state color singlets, and after manipulating integration variables, their contributions to $\bar{H} e^{-S}$ are:

$$\begin{aligned} \bar{H}^{(a1+a2)} &= -16(2\pi)^4 C_B^2 \alpha_s(t_{22}^2) \alpha_s(t_{33}^2) \frac{\xi}{\eta(\xi - \xi_3)} (V(\xi_1 \xi_3 \xi_2) + A(\xi_1 \xi_3 \xi_2) + 2T(\xi_1 \xi_2 \xi_3)) \times \\ &\quad K_0(\sqrt{\xi_2 x m_b^2 \xi \eta b_2}) \left[K_0(\sqrt{\xi_3 x m_b^2 (1 - \xi) \eta b_3}) - K_0(\sqrt{(1 - \xi_3) x m_b^2 \xi \eta b_3}) \right] \end{aligned} \quad (30)$$

$$S^{(a)} = \sum_{i=1}^3 s(\xi_i, \tilde{b}) + \frac{1}{2\beta_1} \left[\log \left[\frac{\log \tilde{t}_2}{-\hat{b}} \right] + \log \left[\frac{\log \tilde{t}_3}{-\hat{b}} \right] + \log \left[\frac{\log \tilde{t}_6}{-\hat{b}} \right] \right] \quad (31)$$

$$\begin{aligned} \bar{H}^{(b1+b2)} &= \frac{64(2\pi)^4 C_B^2 \alpha_s(t_{12}^2) \alpha_s(t_{31}^2)}{(\xi_2 + \xi_3)} \frac{1}{\eta(1 - \xi)} (V(\xi_1 \xi_2 \xi_3) + A(\xi_1 \xi_2 \xi_3) + 2T(\xi_1 \xi_2 \xi_3)) \\ &\quad K_0(\sqrt{(\xi_2 + \xi_3) x m_b^2 \eta b_3}) [K_0(\sqrt{\xi_2 x m_b^2 \xi \eta b_1}) - K_0(\sqrt{\xi_2 x m_b^2 \eta b_1})] \end{aligned} \quad (32)$$

$$\begin{aligned} S^{(b)} &= \sum_{i=1}^3 s(\xi_i, \tilde{b}) + \frac{1}{2\beta_1} \left[\log \left[\frac{\log \tilde{t}_1}{-\hat{b}} \right] + \log \left[\frac{\log \tilde{t}_3}{-\hat{b}} \right] + \log \left[\frac{\log \tilde{t}_4}{-\hat{b}} \right] \right] \end{aligned} \quad (33)$$

$$(34)$$

where

$$t_{1i} = \max[\sqrt{(\xi_2 + \xi_3)xm_b^2\eta}, \frac{1}{b_i}] \quad (35)$$

$$t_{2i} = \max[\sqrt{\xi_2 xm_b^2 \eta \xi}, \frac{1}{b_i}] \quad (36)$$

$$t_{3i} = \max[\sqrt{\xi_3 xm_b^2 \eta (1 - \xi)}, \frac{1}{b_i}] \quad (37)$$

and

$$\tilde{t}_1 = \frac{1}{\Lambda_{QCD}} \max[\sqrt{(\xi_2 + \xi_3)xm_b^2\eta}, \frac{1}{\tilde{b}}] \quad (38)$$

The remaining \tilde{t}_i are defined similarly, as the maximum of \tilde{b}^{-1} and the argument of one of the Bessel functions in the associated \tilde{H} . Here $\beta_1 = \frac{33-2n_f}{12}$, $\tilde{b} = \log(\tilde{b}\Lambda_{QCD})$, and K_0 is the modified Bessel function.

The remaining diagrams are either identically zero due to color algebra, as in the case of the 3-gluon-vertex diagrams, or are suppressed by $\mathcal{O}(\frac{\Lambda_{QCD}}{m_b})$ due to Dirac algebra. Note in particular that all diagrams involving a subtracted heavy quark propagator (henceforth called slashed diagrams) are suppressed by at least $\mathcal{O}(\frac{\Lambda_{QCD}}{m_b})$ with respect to the leading diagrams. It's instructive to contrast this with the meson case to see why. Consider first the meson the two tree-level diagrams are shown in figure [2]. The slashed diagram naively appears suppressed with respect to the other because the heavy quark propagator is $\frac{\gamma \cdot p'}{p'^+ p^-} \sim \mathcal{O}(\frac{1}{m_b})$ whereas the light-quark propagator of the other diagram is $\frac{\gamma \cdot (p' - k)}{-p'^+ k^-}$ which is naively $\mathcal{O}(\frac{1}{\Lambda_{QCD}})$. The p' in the light-quark numerator is eliminated by the final-state spinors, however, leaving $\frac{\gamma \cdot k}{p'^+ k^-} \sim \mathcal{O}(\frac{1}{m_b})$ – the same order as the slashed propagator. For the baryon, consider the diagrams of figure [3]. Analysis of these diagrams is simplified by the fact that their leading terms come from the $g_{\mu\nu}$ pieces of the gluon propagators in this choice of axial gauge. Compare the leftmost quark propagators on the top line. Once again the slashed propagator appears to be suppressed. This time the leading piece p' of the leftmost light-quark propagator in the second diagram is not eliminated, since the adjacent light-quark propagator is offshell and shields it from the final-state spinors. Thus our naive counting of powers of m_b remains correct and the slashed diagram is suppressed with respect to the unslashed diagram, in contrast to the meson case. Combining eqns. (22),(23) with (24)-(28), we may obtain the expression for the form factor $F(x)$. This is the only dynamical difference that we find between the meson and baryon formfactor calculations.

Next we proceed to the calculation of the differential decay rate. Neglecting lepton and proton masses, the differential rate is:

$$\left| \frac{d\Gamma}{dx} \right| = \frac{G_F^2 m_b^5}{96\pi^3} x^2 (3 - 2x) |F(x)|^2 |V_{ub}|^2 \quad (39)$$

To proceed further we need models for the proton and Λ_b wavefunctions. Several models for the proton wavefunction have been proposed in the literature. We adopt the model of Chernyak and Zhitnitskii [16] (neglecting Q^2 evolution):

$$\phi_P^{CZ}(\xi_i, \mu = 1\text{GeV}) = 120\xi_1\xi_2\xi_3[11.35(\xi_1^2 + \xi_2^2) + 8.82\xi_3^2 - 1.68\xi_3 - 2.94 - 6.72(\xi_2^2 - \xi_1^2)] \quad (40)$$

There is little data available on heavy baryon wavefunctions, but some plausible models for Λ -baryons with unequal mass constituents have been proposed from which we choose the following [20]:

$$\phi(\xi, \eta) = N\eta^2(1-\eta)\xi(1-\xi)\exp\left[-\frac{m_b^2}{2\beta^2(1-\eta)} - \frac{m_l^2}{2\beta^2\eta\xi(1-\xi)}\right] \quad (41)$$

N is a normalization constant chosen to fulfill eqn.(26) and m_l is the light constituent quark mass. In the above, β is a parameter related to the string tension and is to be fitted to data. We present results with two typical values for this parameter.

From the form of the distribution amplitudes give above and expressions (28),(30), and (32), we see that there are no remaining singularities from any endpoint regions.

Next the differential decay rate may be evaluated numerically for different values of x . To show the variation of $\frac{d\Gamma}{dx}$ with x , we write it in the form

$$\left|\frac{d\Gamma}{dx}\right| = |V_{ub}|^2 f_{\Lambda_b}^2 f_p^2 R_p(x) \quad (42)$$

$R_p(x)$ is plotted against x for x near 1 in figure [4] for two different values of β , $\beta = 0.5$ GeV (solid line) and $\beta = 1$ GeV (dashed line). In Table I we list the partial decay rates for x integrated from x_1 to x_2 . To get an order of magnitude estimate we use $V_{ub} \sim 0.003$, $f_p = 5.3 \times 10^{-3}$ GeV² [16], and $f_{\Lambda_b} \sim f_p$. The corresponding numerical values for the partial rates are given in the last column of Table I. The total width of Λ_b is approximately 1.6×10^{-12} GeV [21], so that the perturbative partial widths calculated here are of order 10^{-8} of the total Λ_b decay width. This is somewhat smaller than the branching ratios for the analogous meson process $B^0 \rightarrow \pi l^+ \nu_l$ calculated in [4]. We stress, however, that there is considerable uncertainty in the form and parameters of both the Λ_b and proton wavefunctions (see e.g. [22]) and in the value of f_{Λ_b} , which could have considerable impact on our numerical results. Thus our numerical values for the decay rates should only be considered to be rough indicators.

The branching ratio for $\Lambda_b \rightarrow \Lambda_c l \bar{\nu}_l$ is estimated to be approximately 10^{-2} from model calculations [9]. Accounting for the difference in the CKM elements and scaling down from the heavy-heavy decay, we can get an order of magnitude estimate for the branching ratio of $\Lambda_b \rightarrow p l \bar{\nu}_l$ of 10^{-8} , which is consistent with our result given the uncertainties.

We next turn to a discussion of the numerical analysis. We have investigated numerically the contributions of different regions in b -space to determine whether the perturbative contribution is dominant. Following the analysis of [12] we look at the contributions to the form factor $F(x)$ from different parts of the integration region. This is done by checking to see if the dominant contribution comes from the small- b regions of b -space. We check this numerically by cutting off the each of the b -integrals at some maximum b_c , i.e $b_1, b_2, b_3 < b_c$. Our results are shown in figure [5] for $\beta = 1$ GeV. We observe that for $\Lambda_{QCD} b_c > 0.8$ the value of $F(x)$ is essentially constant, indicating that most of the contribution to the integral comes from the region $b_1, b_2, b_3 < \frac{0.8}{\Lambda_{QCD}}$. The curves with the largest values of x appear to flatten more quickly than the smaller- x curves at large b_c , indicating that for more energetic outgoing protons the perturbative regime is more dominant than that of less energetic ones, as expected.

Following [12], we may define $b_{1/2}$ to be the value of b_c at which 50% of the total value of $F(x)$ has been accumulated. A loose criterion proposed for the consistency of perturbation theory that $\alpha_s^2(\frac{1}{b_{1/2}}) < 1$. Our result satisfies this criterion: for $x = 1, \beta = 0.5$ GeV, $b_{1/2}$ is 0.40 and $\alpha_s = 0.83$. Other x and β tested give larger values of $b_{1/2}$, but even the case $\beta = 1.0$ GeV, $x = 0.75$ gave $\alpha_s = 0.91$. This indicates that most of the value of $F(x)$ is accumulated in the short-distance region of the integration space in which we may expect the perturbative expansion to be self-consistent.

In this paper we have calculated the perturbative contribution to the decay $\Lambda_b \rightarrow p l \bar{\nu}_l$ to leading order in $\frac{1}{m_b}$. This is the dominant contribution as $m_b \rightarrow \infty$, and we have investigated the self-consistency of the perturbative approach for realistic values of m_b . With our choice of model wavefunctions for the heavy baryon and proton we find that the perturbative contribution of $\Lambda_b \rightarrow p l \bar{\nu}_l$ to the total width of Λ_b is of order 10^{-8} of the total width. Our confidence in the self-consistency of the the result is supported by the fact that the largest contribution to the form factor comes from the short-distance regions of the integration space, as discussed above. We stress again that there is considerable uncertainty in the numerical results due to uncertainty about the wavefunctions. However, for at least one plausible set of model wavefunctions we obtain values for the decay rates comparable to those calculated for $B^0 \rightarrow \pi l^+ \nu_l$ using a perturbative expansion made consistent by the introduction resummed Sudakov effects. The issue of the contributions from higher orders in $\frac{1}{m_b}$ (higher twist) is beyond the scope of this paper.

We are very grateful to George Sterman for many helpful conversations and useful suggestions. We would also like to thank Graham Kribs for help with the computer programming. One of us (R.A.) would like to thank the Service Physique Theorique, Saclay, for hospitality and support. This work was supported in part by the U.S. Department of Energy.

References

- [1] M. Bauer, B. Stech, and M. Wirbel, Z. Phys. C **29**, 637 (1985); B. Grinstein, N. Isgur, and M.B. Wise, Phys. Rev Lett. **56**, 298 (1986); M. Bauer and B. Stech, Z. Phys. C **42**, 671 (1989); B. Grinstein, N. Isgur, D. Scroba, and M.B. Wise, Phys. Rev. D **39**, 797 (1989); P. Ball, V.M. Braun, H.G. Dosch, Phys. Lett. B **273**, 316 (1991); V.M. Belyaev, A. Khodzhamirian, R. Ruckl, Z. Phys. C **60**, 349 (1993).
- [2] G. Altarelli, N. Cabibbo, G. Corbo, L. Maiani, and G. Martinelli, Nucl. Phys. **B208**, 365, (1982); J.L. Rosner, Phys. Rev. D **42**, 3732 (1990).
- [3] N. Isgur and M.B. Wise, Phys. Lett. B **232**, 113 (1989); **237**, 527 (1990); H.D. Politzer and M.B. Wise, *ibid.* **206**, 681 (1988); **208**, 504 (1988); M.B. Voloshin and M.A. Shifman, Yad. Fiz. **45**, 463 (1987) [Sov. J. Nuc. Phys]. **45**, 511 (1987)]; E. Eichten and B. Hill, Phys. Lett. B **234**, 511 (1990); **243**, 427 (1990); B. Grinstein, Nucl. Phys. B

339, 253 (1990); A.F. Falk and B. Grinstein, Phys. Lett. B **247**, 406 (1990); **249**, 314 (1990).

[4] R. Akhoury, G. Sterman, and Y-P Yao, Phys. Rev. D **50**, 358 (1994).

[5] H. Georgi, Phys. Lett. B **240**, 447 (1990); A. Falk, H. Georgi, B. Grinstein, and M.B. Wise, Nucl. Phys. **343**, 1 (1990).

[6] H-N Li and H-L Yu, [hep-ph/9411308](#).

[7] A.H. Mueller, Phys. Rev. D **20** 2037 (1979); J.C. Collins, *ibid.* **22** ,1478 (1980); A. Sen, *ibid.* **24**, 2181 (1981); G.P.Korchemskii and A.V. Radyushkin, Yad. Fiz. **45**,1466 (1987) [Sov. J. Nucl. Phys. **45**, 910 (1987)].

[8] A.V.Efremov and A.V.Radyushkin, Phys. Lett. B **94**, 245 (1980); G.P. Lepage and S.J. Brodsky, Phys. Rev. D **22** 2157 (1980); Phys Lett. B **87**, 359 (1979); Phys. Rev. Lett. **43**, 545 (1979).

[9] R. L. Singleton, Phys. Rev. D **43**, 2939 (1991).

[10] M. Jimack, talk at XXX Rencontres de Moriond (1995), to be published in the proceedings.

[11] H-N Li and G. Sterman, Nucl. Phys. B **381** 129 (1992).

[12] H-N Li, Phys. Rev. D **48** 4243 (1993).

[13] J. Botts and G. Sterman, Nucl. Phys. B **325** 62 (1989).

[14] J. Bolz, R. Jakob, P. Kroll, M. Bergmannn, and N.G. Stephanis, [hep-ph/9405340](#).

[15] R. Akhoury and W. Loinaz, in preparation.

[16] V.I. Chernyak and I.R. Zhitnitsky, Nucl. Phys. B **246** 52 (1984).

[17] I.D. King and C.T. Sachrajda, Nucl. Phys. B **279** 785 (1987).

[18] F. Hussain, J.G. Korner, M. Kramer, G. Thompson, Z. Phys. C **51** 321 (1991).

[19] R. Akhoury and I. Z. Rothstein, Phys. Lett. B **337** 176 (1994).

[20] F. Schlumpf, [hep-ph/9211255](#).

[21] Particle Data Group, Phys. Rev. D **50**, 1173 (1994).

[22] R. Eckardt, J. Hansper, M.F. Gari, Z. Phys. A **350** 349 (1995).

Figure Captions

Figure 1 Leading Tree-Level Diagrams in Spacelike Axial Gauge

Figure 2 Tree-level Diagrams for $B^0 \rightarrow \pi l^+ \nu_l$

Figure 3 A Suppressed Diagram and a Leading Diagram

Figure 4 $R_p(x)$ vs. x for $\beta = 1$ GeV (dashed line) and $\beta = 0.5$ GeV (solid line). $R(x)$ is in units of GeV^{-7}

Figure 5 $40F(x)$ vs. b_{cutoff} for $\beta = 1$ GeV. The curves are $x = 0.75, 0.8, 0.85, 0.9, 0.95, 1.0, \frac{1}{\Lambda_{QCD}}$ intersecting the $b = 1$ line from top to bottom respectively. b_{cutoff} is in units of

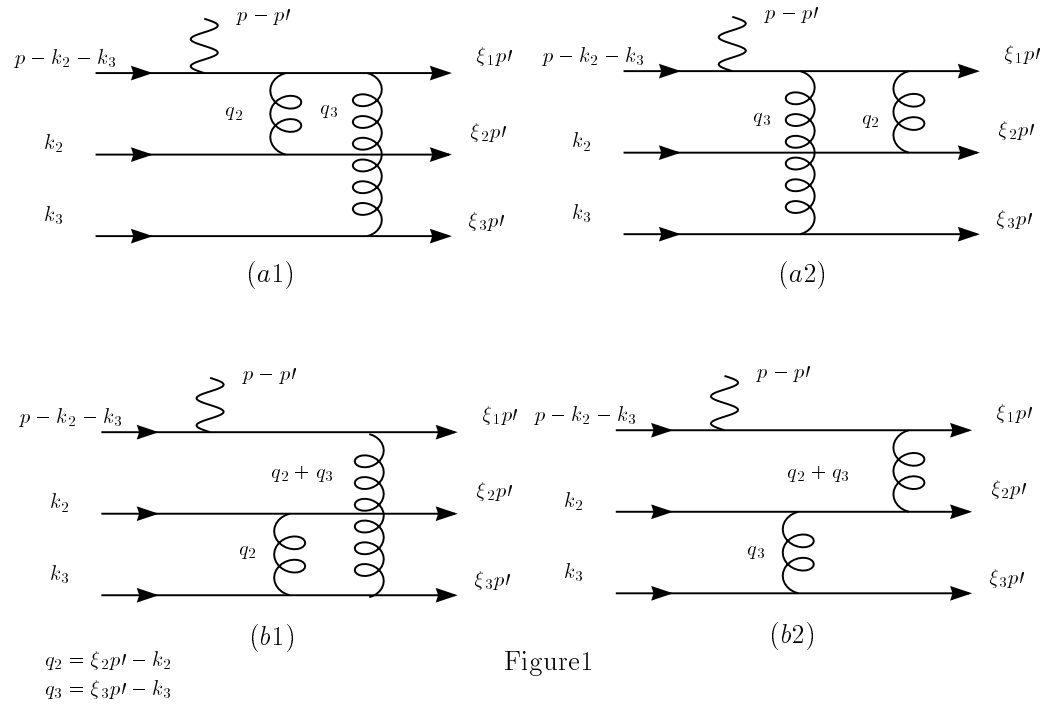


Figure 1

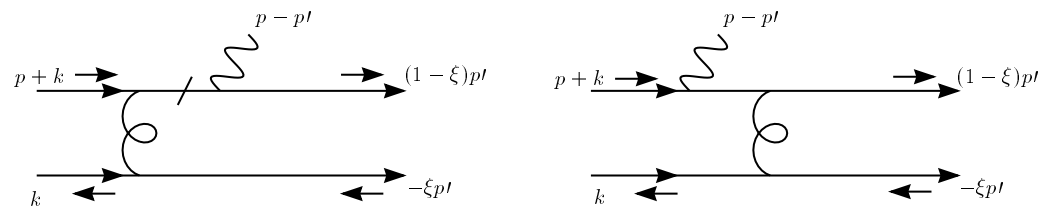


Figure2

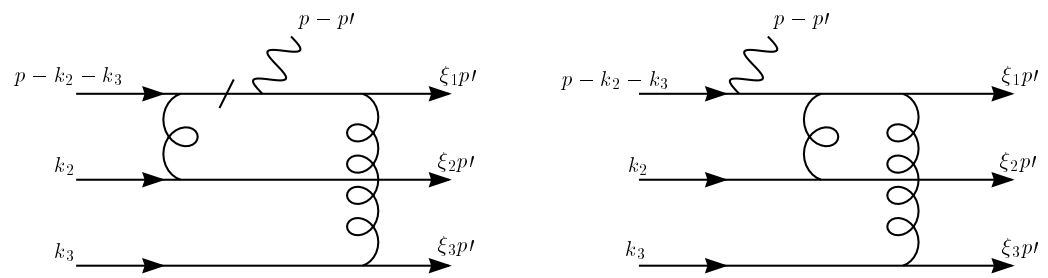


Figure3

Figure 4

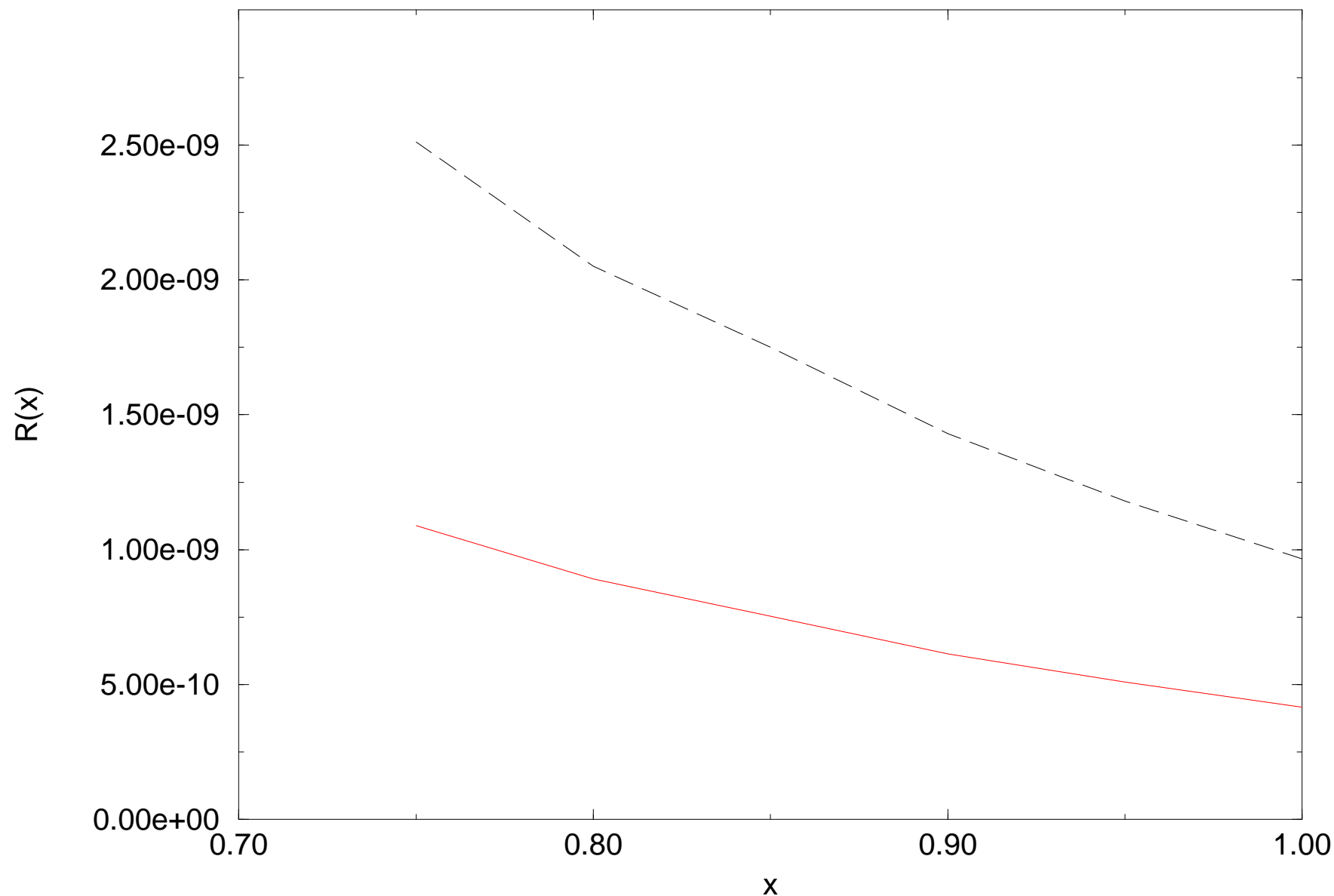


Figure 5

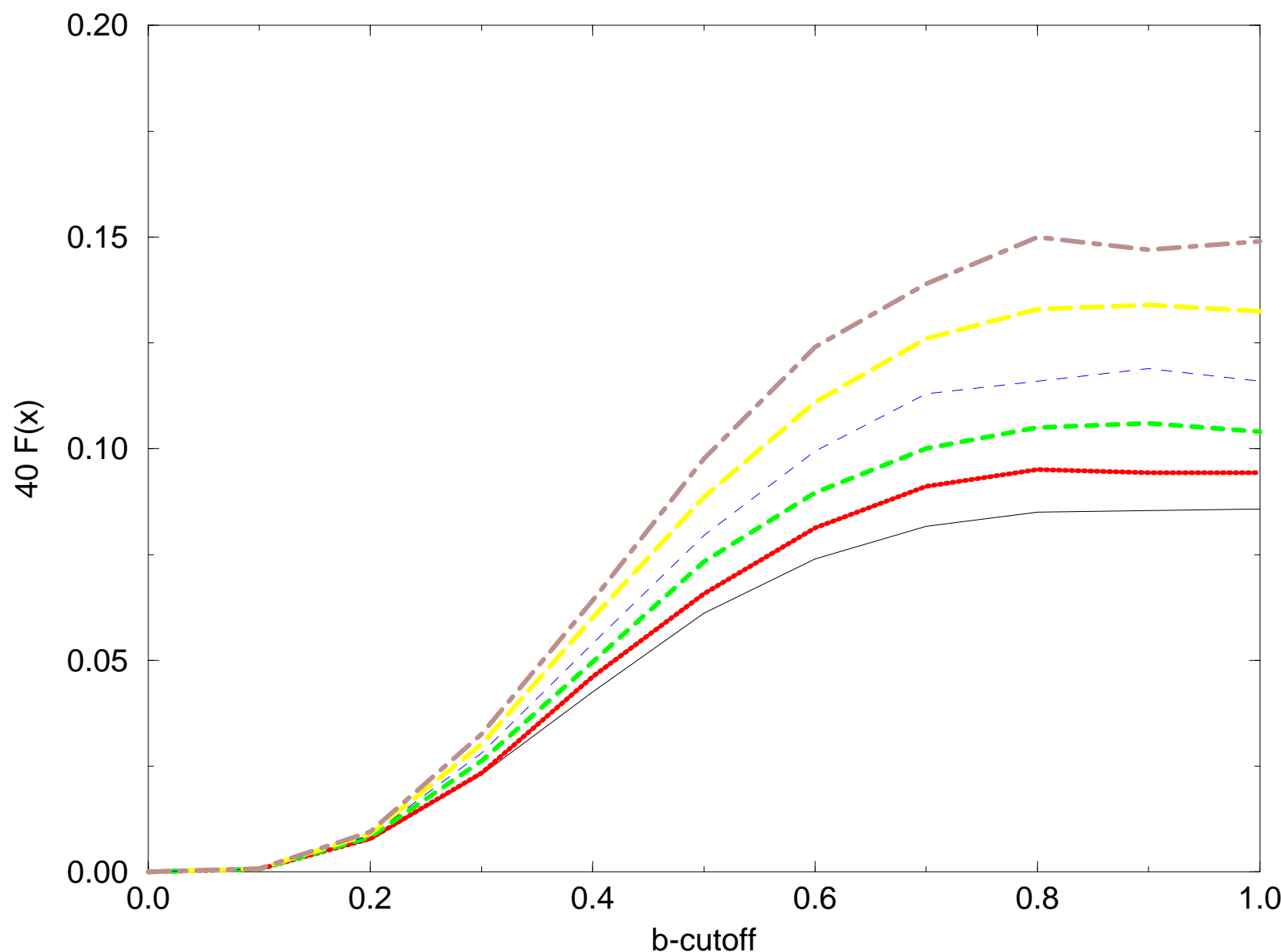


Table 1.

Process	x_1	x_2	$\Gamma_{\text{theory}}^{\text{partial}}(\text{GeV})$	$\Gamma_{\text{theory}}^{\text{partial}}(\text{GeV})$
			$\beta = 1 \text{ GeV}$	$\beta = 0.5 \text{ GeV}$
$\Lambda_b \rightarrow p l \bar{\nu}_l$	0.75	1.0	2.4×10^{-21}	5.7×10^{-21}
	0.85	1.0	1.1×10^{-21}	2.8×10^{-21}
	0.75	0.90	1.7×10^{-21}	4.1×10^{-21}